Mach 6 Tests of Scramjet Engine with Boundary-Layer Bleeding and Two-Staged Injection

Masatoshi Kodera, Sadatake Tomioka, Kan Kobayashi, Takeshi Kanda and Tohru Mitani

Japan Aerospace Exploration Agency
1-Koganezawa, Kimigaya, Kakuda, Miyagi 981-1525
kodera.masatoshi@jaxa.jp

Keywords: Scramjet, Boundary-layer bleeding, Staged fuel injection

Abstract

In this study, a boundary-layer bleeding and a two-staged fuel injection were applied to a scramjet engine for suppressing unstart transition and improving the thrust performance under Mach 6 flight conditions. With the boundary-layer bleeding, the engine could operate without unstart transition around at the fuel equivalence ratio of unity (Φ=1). The thrust increment from the no fuel condition (*dF*) increased to 2460 N, which was about 1.4 times as large as that of the case without the bleeding and maximum in our Mach 6 tests. It was confirmed that the boundary-layer bleeding suppressed the separation during the engine operation. The two-staged fuel injection was less effective for improving the thrust performance compared with the single-staged one with the bleeding at Mach 6.

Introduction

Scramjet engine is expected to be a main engine for the aerospace plane, which is a future space transportation system. Japan Aerospace Exploration Agency (JAXA) has been conducting firing tests of a variety of sub-scale scramjet engines in Mach 4, 6, 8 simulated flight conditions using Ramjet Engine Test Facility (RJTF) [1]-[5].

In a series of these tests, the engine produced the thrust over the engine drag. However under the low Mach number conditions such as 4 and 6, the obtained results were insufficient because the engine unstart was induced by a boundary layer separation in the combustor at a small fuel equivalence ratio (Φ) less than unity.

The combustion induced pressure rise in the combustor propagated upstream through the separation. When the pressure rise was beyond a separation limit around the inlet exit, it traveled upstream toward the inlet. This is so-called combustor-inlet interaction (CII) [6]. Then the engine performance became much worse. Such a engine condition is called unstart.

To prevent CII, the extension of the isolator length was tested at Mach 4 and 6 [1][2]. Indeed it was confirmed that the longer isolator suppressed it. However there is a limit to its length to realize a combustor of reasonable size. Therefore alternative ways of controlling CII must be considered.

In this study, under the Mach 6 flight conditions we tried to apply a boundary-layer bleeding to the engine previously tested [2] in order to suppress CII and to improve the thrust performance by increasing Φ up to unity. The boundary-layer bleeding was already tested under the Mach 4 flight conditions [4]. In this test, we succeeded in increasing the maximum thrust. This result is a motivation for the present study.

Indeed the bleeding is expected to be effective for suppressing CII. However there is a problem for its practical use because the bled gas temperature is too high to handle it easily especially for the Mach 6 case. Therefore we also tested a staged fuel injection as another way to suppress CII instead of the bleeding.

The combustor comprises a constant-area section followed by a diverging-area section. For the staged fuel injection, some fuel is injected in the constant-area section under the condition without CII and the remainder is injected in the diverging-area section. Although the fuel injection only in the constant-area section yields the maximum thrust performance, it may be better for the staged injection if the amount of the fuel is larger without CII [7]. In fact, the maximum thrust for a two-staged injection was comparable to that for a single-staged injection with the bleeding under the Mach 4 conditions [4].

In this paper, we will discuss the effects of the bleeding and the two-staged injection on the thrust performance and the flowfields in the engine by using measured thrust and wall pressure data.

Experimental apparatus

RJTF

The combustion tests have been carried out under the Mach 6 simulated flight conditions using RJTF, which is a free-jet type high enthalpy wind tunnel with a rectangle nozzle of 510 mm×510 mm. The engine entrance conditions assuming the stream after passing the forebody shock wave at Mach 6 is indicated in Table 1. To obtain a high total temperature flow, a storage air heater is used. The velocity boundary layer thickness at the nozzle exit was evaluated from pitot pressure measurements. Further details of RJTF are described in Ref. [8].

Table 1: Test conditions of Mach 6 at RJTF

Mach number	5.3
Stagnation pressure (MPa)	4.8
Stagnation temperature (K)	1450
Boundary layer thickness (mm)	58

Engine

Figure 1 shows a schematic view of the sub-scale engine tested in this study. The engine has a side wall compression inlet and a side wall expansion nozzle swept back at 45 degrees. The engine walls consist of two side walls, a top wall and a cowl. The overall length, height and width of the engine are 2100 mm, 250 mm and 200 mm, respectively. A strut with the same height as the flow path was installed in the engine to enhance the combustion.

The geometrical contraction ratio of inlet, which is the area of the inlet entrance to that of the inlet exit, is approximately 3 without the strut. The cowl leading edge is located at the inlet exit to allow the spill of the incoming air into the external flows to the engine for better starting characteristics. An isolator of 200 mm in length between the inlet and the combustor is set up for avoiding the influence of the pressure increase in the combustor on the inlet flow. The backward facing steps of 4 mm in height on the side walls between the isolator and the combustor are used for flame holding. The combustor consists of the constant-area combustor (C. C.) and the diverging-area combustor (D. C.).

Fuel injection

Main fuel injectors (MV1 and MV2) are located at 30 and 16 mm downstream of the step in the C. C. section and second-stage fuel injectors (MV3) used for the two-staged fuel injection are located at 558 mm downstream of the step in the D. C. section. MV3 was designed for the ramjet mode operation [9] in the first time, not for the staged injection. Fuel hydrogen is normally injected at sonic speed from 12 orifices with a diameter of 1.5 mm for the main injectors and 6 ones with a diameter of 2.1 mm for the second-stage injectors on each side wall. The vertical distances between the adjacent orifices are 20 and 40 mm for the main and second-stage injectors respectively. In this paper, we do not discriminate between MV1 and MV2 because there were no significant differences between the results with the both injectors. The fuel mass flow rate (m_f) of 145 g/s corresponds to Φ of unity assuming the air capture ratio of 0.8 obtained by CFD [10].

Ignition

A torch-igniter (TI) was installed on the top wall 20 mm upstream of the step to ignite stably in the Mach 6 conditions, which are near a lower temperature limit of self-ignition. In TI, a high temperature gas is generated by combustion of a mixture gas of hydrogen and oxygen at the equivalence ratio of 2.1. The combustion gas is exhausted from TI at the mass flow rate of 3 g/s and the chamber pressure of 630 kPa. The details of TI are described in Ref. [4].

Boundary-layer bleeding

The boundary layer is bled through porous holes opened on the top wall around the inlet exit at the mass flow rate of 30 g/s, which is only 0.5 % of the inflow mass flow rate at the inlet entrance. The details of the bleeding device and operation are described in Ref. [11].

Scramjet engine is supposed to be integrated with a fuselage because it is utilized as a part of engine components such as compression and expansion surfaces to reduce the total weight of integrated system. There-

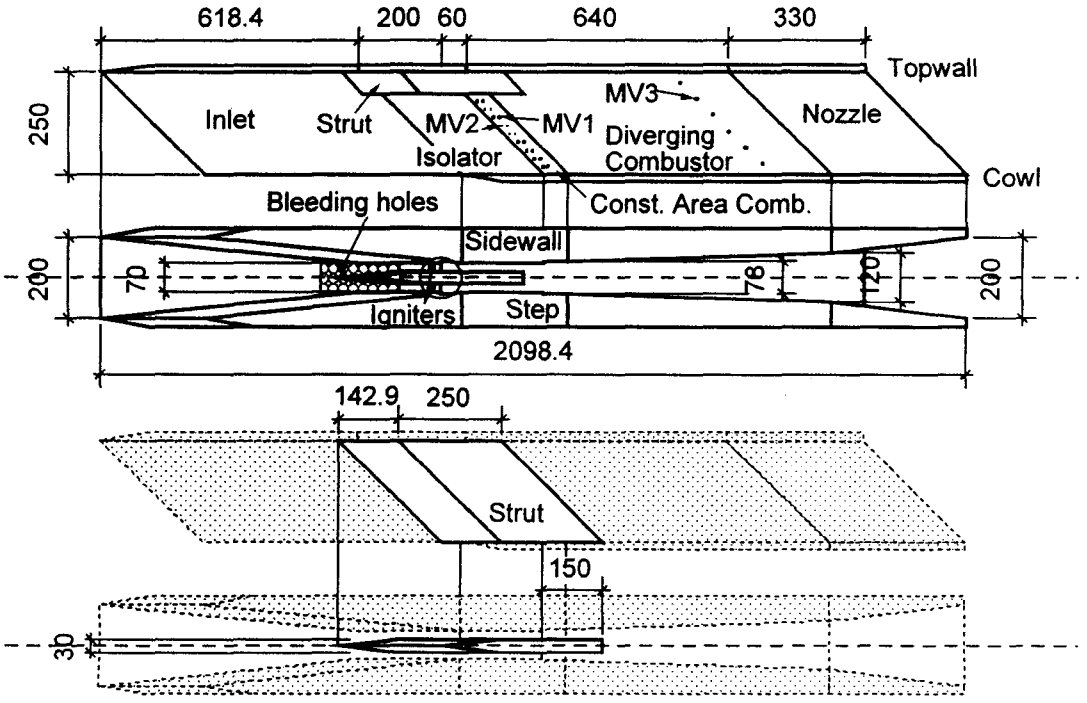

Fig. 1: Schematic views of a scramjet engine model

fore the inlet ingests a thick boundary layer developed on the fuselage wall. RJTF gives the thick boundary layer developed on the facility nozzle wall into the top wall side of the inlet entrance to simulate such a condition. As a result, a large boundary layer separation easily occurs in the engine on the top wall. Therefore we applied the bleeding to the top wall boundary layer.

Measurements

The thrust was measured by means of a force measurement system (FMS). Its measurement error was ± 50 N. The wall pressure was also measured at 170 ports on the top wall, the side wall and the cowl.

In this test, m_f was varied every 2 seconds. Sometimes the flowfields in the engine changed at a certain m_f within 2 seconds because the wall temperature increased. In this case, two results at the same m_f will be shown in the figures on FMS and the pressure later.

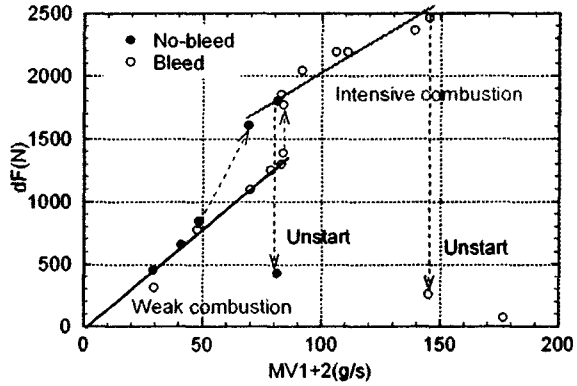

Fig. 2: Thrust increment from no fuel condition

Results and discussions

Test with boundary-layer bleeding

Thrust performance Figure 2 shows the thrust increment from the no fuel condition (dF) versus m_f in the cases with and without the boundary-layer bleeding. The fuel is injected from the main injectors.

In this figure, dF increased steadily with increasing m_f. However dF jumped suddenly to a higher level beyond a certain m_f. Here we could observe two typical combustion modes, which were reported in our previous tests and called "weak combustion" and "intensive combustion" [2]. With further increasing m_f, dF dropped drastically to a much lower level and the engine went into unstart.

Without the bleeding, unstart transition occurred at m_f=80 g/s, which was a small additional amount of m_f after changing to the intensive combustion mode at m_f=70 g/s, and then dF was limited to 1800 N. Here m_f at unstart transition is termed "unstart point".

On the other hand, with the bleeding, the engine operated without unstart transition at up to m_f=145 g/s, which corresponded to Φ=1. As a result, we could achieve the purposes of this study, that is, the boundary-layer bleeding suppressed unstart transition and dF increased to 2460 N, which was about 1.4 times as large as that of the case without the bleeding and

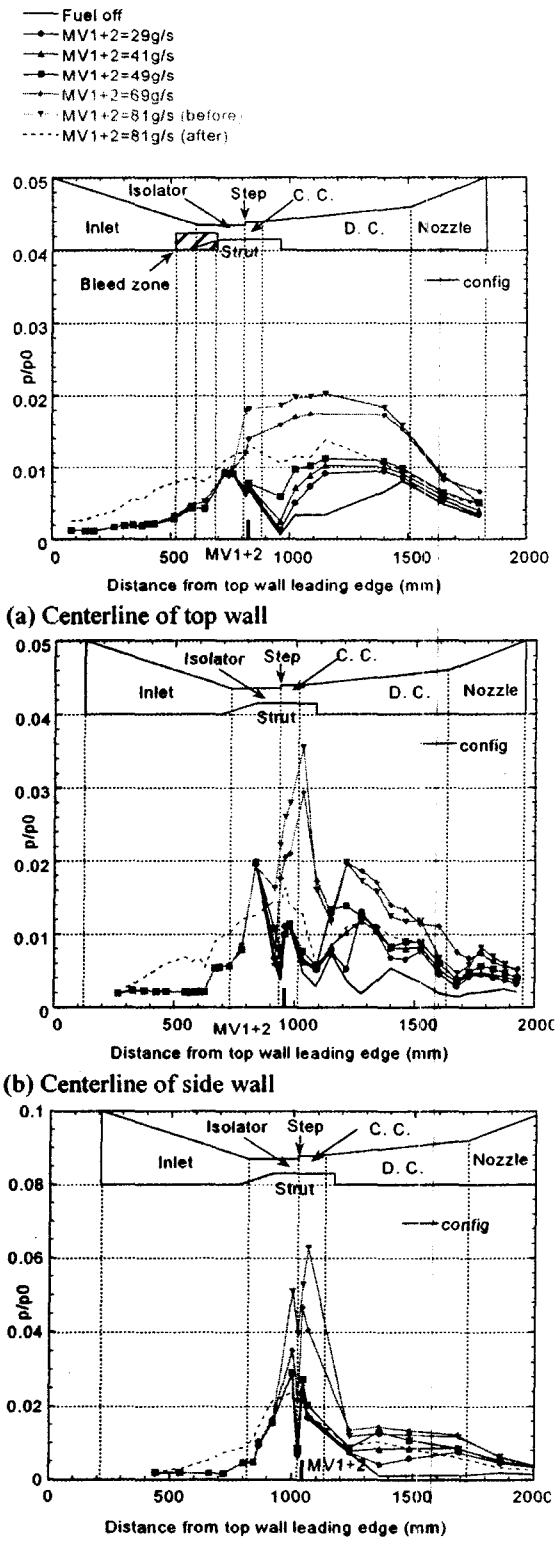

Fig. 3: Wall pressure distributions without boundary-layer bleeding

maximum in our Mach 6 tests. On the other hand, m_f at the transition from weak to intensive combustion was larger with the bleeding.

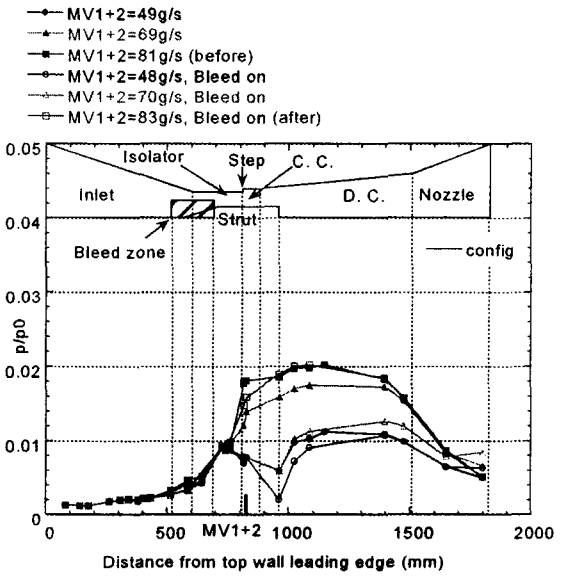

Fig. 4: Wall pressure distributions along centerline of top wall (Comparison between cases with and without boundary-layer bleeding)

Wall pressure variations without bleeding Figure 3 shows the wall pressure distributions along (a) the centerline of the top wall, (b) the centerline of the side wall and (c) the horizontal line close to the cowl on the side wall without the bleeding. Note that the top wall pressure data in the location of the strut was sampled along a line between the side wall and the strut surface. Pressures are normalized by the total pressure of the incoming free stream.

As mentioned before, the result changed at a certain m_f within the measured time (2 seconds). In this case, the results before and after the change are indicated as "before" and "after" respectively in the figure. The horizontal section of the half engine flow path corresponding to each distribution is also shown as "config" at the top of the figure. These expressions are used for all figures on the pressure distributions.

When the fuel was not injected, a higher pressure was observed on the top wall around the D. C. exit because of the impingement of the shock wave emanated from the cowl leading edge (cowl shock) as shown in Fig. 3 (a). Around this region, the combustion initiated with a small boundary layer separation by injecting the fuel because the fuel was concentrated around the top wall downstream of the combustor, as described in Ref. [2][12]. Then, the mutual interaction occurred between the growth of the separation area and the fuel/air mixing and combustion within it. However at m_f=30 g/s, the pressure increased locally in the D. C. section due to the precombustion shock by this interaction. This is a typical pressure distribution in the weak combustion mode. With increasing to m_f=50 g/s, the pressure rise by the combustion moved upstream with the enlargement of the separation on the top wall, while the increase in the pressure level was relatively small.

With further increasing to m_f=70 g/s, the influence of the combustion in the D. C. section reached to the C. C. section near the top wall resulting in the combustion. This combustion spread over the whole C. C. section toward the cowl. Then the pressure became much higher in the C. C. section. Simultaneously the combustion occurred even around the strut base near the top wall. Consequently the pressure on the top wall in the D. C. section was so high that the combustion changed to the intensive mode.

In the intensive combustion mode, the extremely higher pressure region was observed near the cowl in the C. C. section. The combustion around this region caused the boundary layer separation on the side wall that propagated upstream of the step in the isolator and induced unstart transition as described in Ref. [1]. At m_f=80 g/s, the intensive combustion was maintained only for about 1 second. After that, the pressure increased over the whole inlet section. This is a typical pressure distribution after unstart transition.

Comparison between cases with and without bleeding Figure 4 shows the comparison of the pressure distributions along the centerline of the top wall between the cases with and without the bleeding.

From the figure, it was found that the location of the pressure rise due to the combustion in the case of the bleeding was more downstream of that without the bleeding at the same m_f, in the weak combustion mode. In addition, the transition to intensive combustion mode happened at the larger m_f with the boundary-layer bleeding. This proved that the transition from weak to intensive combustion mode was controlled by the enlargement of the separation on the top wall as explained before. That is to say, the upstream extension of the separation on the top wall was reduced by bleeding the top wall boundary layer.

Once changed to the intensive combustion mode, the pressure distributions with and without the bleeding were almost the same as well as the thrust performances, except for the pressure levels around the step.

Figure 5 shows the pressure distributions with the bleeding at m_f beyond the unstart point in the case of no bleeding. With increasing m_f, the pressure steadily increased in the combustor except for the region near the cowl in the D. C. section. On the other hand, the pressure rise propagated upstream of the step in the isolator through the separation on the side wall. This upstream extension increased as going closer to the cowl due to the higher back pressure. At m_f=145 g/s, the pressure rise was observed near the inlet exit on the cowl side, while it was not observed even in the middle of isolator on the top wall. This pressure distribution was held only for about 1 second and then shifted to unstart. This proved that unstart transition did not occur until the boundary layer separated from the top wall near the inlet exit.

Next, we considered the pressure limit without the separation around the inlet exit on the top wall, p_s. Here we paid attention to the maximum pressures on the top wall in the C. C. section just before unstart

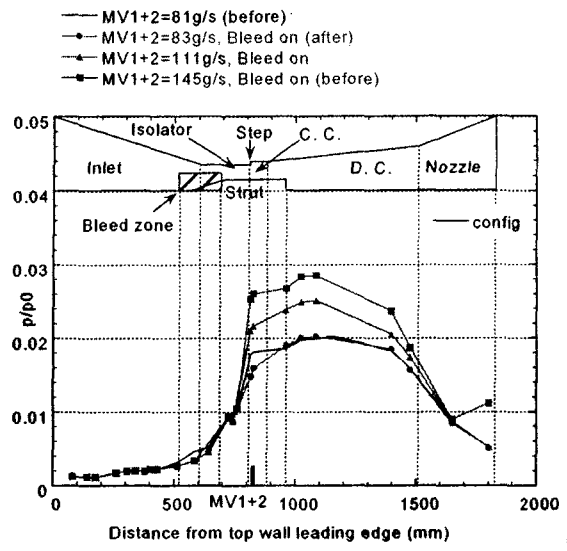

a) Centerline of top wall

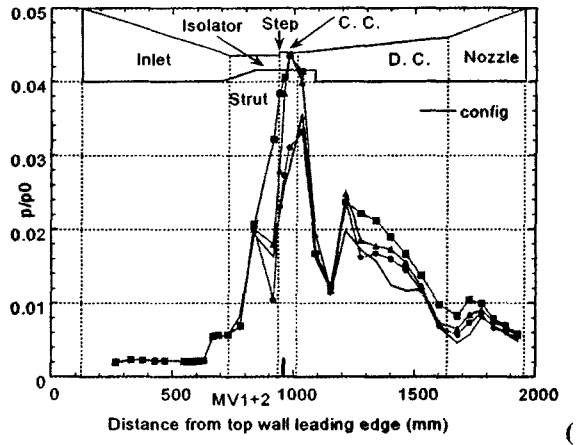

b) Centerline of side wall

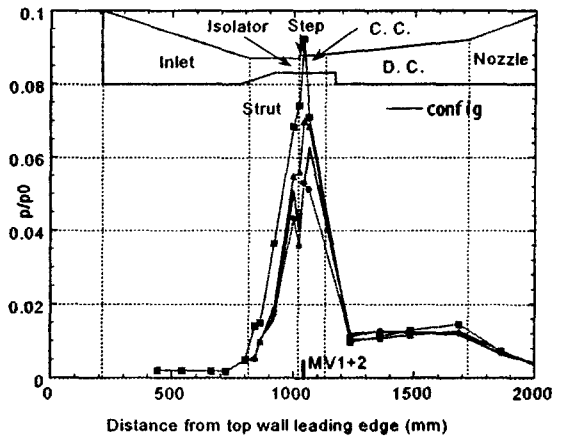

(c) Line close to cowl on side wall

Fig. 5: Wall pressure distributions with boundary-layer bleeding beyond unstart point without bleeding

transition for the cases with and without the bleeding. The maximum pressure approximately equals to p_s. Note that since the maximum pressure is selected in the available data, the selected pressure value may be not really maximum. From Fig. 5, the normalized p_s without the bleeding was 0.018, while that with the bleeding was 0.026. Hence it was found that the boundary layer with the bleeding was able to withstand the steeper adverse pressure gradient by the combustion without the separation, even if the amount of bled air was very small.

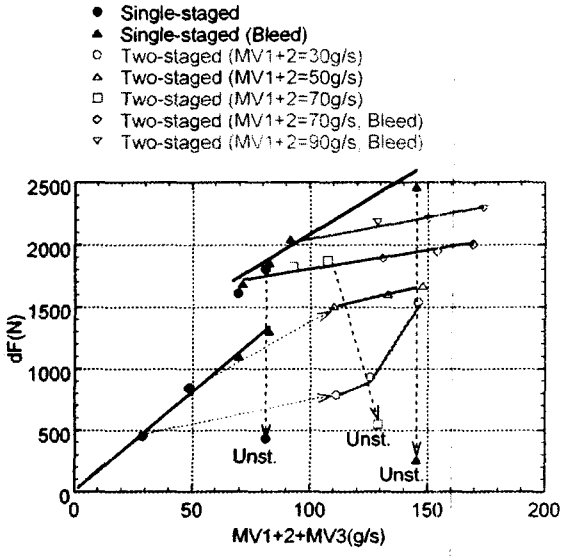

Fig. 6: Thrust increment from no fuel condition by applying two-staged fuel injection

Test with two-staged fuel injection

Thrust performance Figure 6 shows dF versus the total m_f ($m_{f,\,total}$) for the two-staged fuel injection. The results for the single-staged fuel injection are also shown in this figure for the comparison. Here MV1 and MV2 in the C. C. section, and MV3 in the D. C. section are used for the first-stage fuel injectors and the second-stage ones respectively. m_f at the first-stage (m_{f1}) is fixed at 30, 50, 70, 90 g/s and that at the second-stage (m_{f2}) is increased. At m_{f1}=30 and 50 g/s, the boundary-layer bleeding was not applied because of no unstart transition. At m_{f1}=70 g/s without the bleeding, unstart transition occurred when m_{f2} was slightly injected. Then, at m_{f1}=70 and 90 g/s, the boundary-layer bleeding was applied. For the single-staged fuel injection with the bleeding, the combustion modes at m_{f1}=70 and 90 g/s were weak and intensive respectively. To change to intensive combustion at m_{f1}=70 g/s, m_{f1} was decreased to 70 g/s after the fuel injection at m_{f1}=90 g/s. Then, the intensive combustion was maintained.

In Fig. 6, dF for the two-staged fuel injection was lower than that for the single-staged fuel injection with the bleeding at the same total fuel flow rate. When the combustion mode was intensive only by the first-stage fuel injection at m_{f1}=70 and 90 g/s, the second-stage fuel injection was not effective for the thrust increment. There was no significant increment of dF by the combustion with increasing m_{f2}. On the other hand, when the combustion mode was weak only by the first-stage fuel injection at m_{f1} = 30 and 50 g/s, dF

suddenly increased with increasing m_{f2} at a certain $m_{f,\,total}$. At m_{f1}=30 g/s and m_{f2}=120 g/s, a thrust jump was observed. It was expected that such a thrust jump occurred even at m_{f1}=50 g/s and $m_{f,\,total}$<100 g/s, though the data were not available in this test. At m_{f1}=50 g/s and $m_{f,\,total}$>100 g/s, the change of dF with $m_{f,\,total}$ was very small.

Wall pressure variations with two-staged injection

Figure 7 and 8 show the wall pressure distributions of the two-staged fuel injection at m_{f1}=30 and 70 g/s respectively.

At m_{f1}=70 g/s, it was observed that the pressure around the second-stage fuel injector slightly increased with increasing m_{f2}. However there was no remarkable change producing the large thrust increment for the wall pressure distributions. When the combustion mode was intensive, the region close to the wall around MV3 was filled with the unburned fuel and the reactants flowing from the upstream combustion region especially near the top wall, where the principal combustion occurred [2]. Therefore the pressure could hardly increase in the engine by using the second-stage fuel injection. This result was similar to that in a test of a staged supersonic combustor with two-staged wall injections [13]. Note that around MV3 near the cowl, the residence time of fuel and air was shorter without the separation, though the air relatively existed.

At m_{f1}=30 g/s, the change of the wall pressure distributions with increasing m_{f2} was different from that at m_{f1}=70 g/s. At m_{f1}=30 g/s and m_{f2}<100 g/s, the pressure rise was observed around MV3, but it was small. However at m_{f1}=30 g/s and m_{f2}=120 g/s, the pressure increased largely, because the pressure rise around MV3 propagated upstream and the combustion occurred around the strut trailing edge. At that time, the pressure near the step did not increase yet. The larger pressure rise such as the intensive combustion might occur at m_{f1}=30 g/s and m_{f2}>120 g/s, if the combustion occurred near the step. From the case at m_{f1}>50 g/s, it was supposed that once the intensive combustion occurred, there was no significant change with increasing m_{f2} for the pressure distributions.

As mentioned before, the thrust performance for the two-staged fuel injection was worse than that of the single-staged fuel injection with the bleeding. This means that the boundary-layer bleeding is better for our purposes so far. This is possible to be due to that the spanwise arrangement as well as the streamwise location of the fuel injectors were not optimized. Therefore we plan to investigate these points in the next RJTF test.

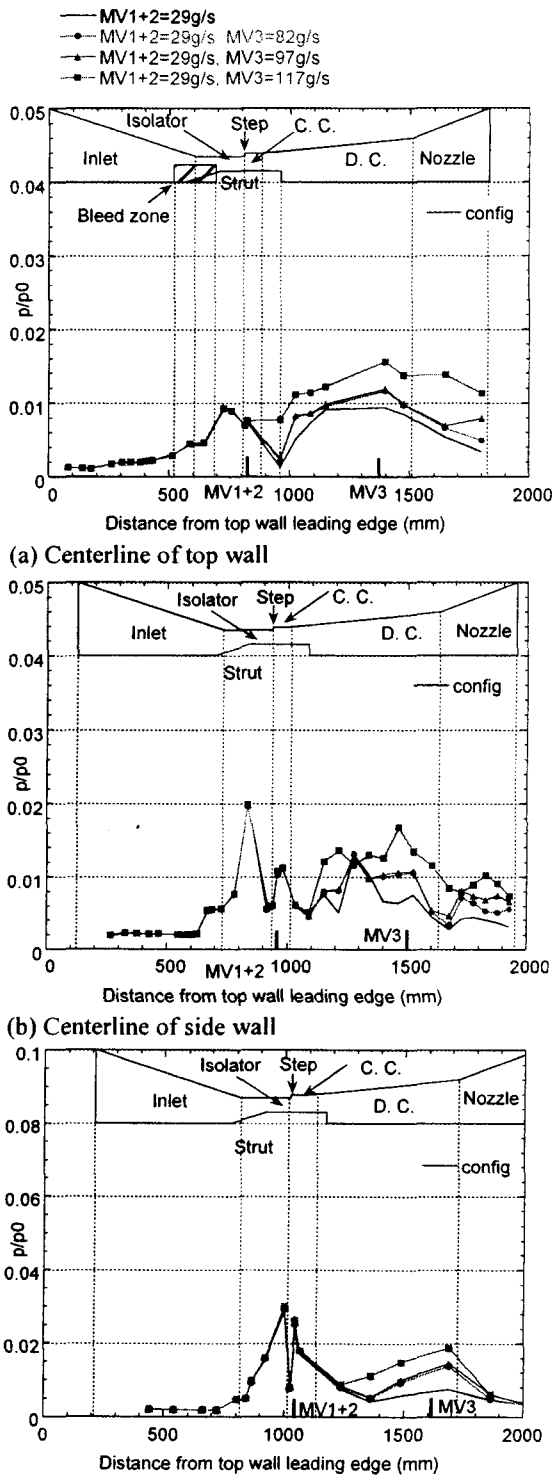

Fig. 7: Wall pressure distributions of two-staged fuel injection at first-stage fuel flow rate of 30 g/s

Conclusion

Mach 6 tests of a scramjet engine model were carried out at RJTF and the effects of the boundary-layer bleeding and the two-staged fuel injection on suppressing CII causing unstart transition and improving the thrust performance were analyzed. The following results were obtained.

1) By applying the boundary-layer bleeding, the engine operated without unstart transition around at

the fuel equivalence ratio (Φ) of 1. The thrust increment from the no fuel condition (dF) increased to 2460 N, which was about 1.4 times as large as that without the bleeding and maximum in our Mach 6 tests.

2) With the bleeding, the transition from weak to intensive combustion was delayed and the pressure limit to the separation increased. These confirmed that the boundary-layer bleeding suppressed the separation.
3) The two-staged fuel injection was less effective for improving the thrust performance compared with the single-staged fuel injection with the bleeding under the Mach 6 conditions.

References

1) Sunami, T., Sakuranaka, N., Tani, K., Hiraiwa, T., and Shimura, T., "Mach 4 Tests of a Scramjet Engine -Effects of Isolator," *Proceedings of 13th ISABE 97-7088*, 1997.
2) Sato, S., Izumikawa, M., Tomioka, S., and Mitani, T., "Scramjet Engine Test at Mach 6 Flight Condition," AIAA Paper 97-3021, 1997.
3) Kanda, T., Wakamatsu, Y., Ono, F. and Izumikawa, M., "Mach 8 Testing of a Scramjet Engine Model, " AIAA 99-0617.
4) Kobayashi, K., Tomioka, S., Hiraiwa, T., Kato, K., Kanda, T. and Mitani, T., "Suppression of Combustor-Inlet Interaction in a Scramjet Engine under M4 Flight Condition," AIAA Paper 2003-4737, 2003.
5) Hiraiwa, T., Kanda, T., Mitani, T. and Enomoto, Y., "Experiments on a Scramjet Engine with Ramp-Compression Inlet at Mach 8 Condition," AIAA Paper 2002-4129.
6) Billig, F. S., "Research on Supersonic Combustion," *Journal of Propulsion and Power*, Vol. 9, No. 4, July-Aug. 1993.
7) Billig, F. S., "Combustion Processes in Supersonic Flow," *Journal of Propulsion*, Vol. 4, No. 3, May-June 1988.
8) Hiraiwa, T., et al., "Calibration Studies of Nozzle Flow in Ramjet Engine Test Facility," 11th International Symposium on Space Technology and Science, 96-d-14, 1996.
9) Kato, K., Kanda, T., Kudo, K., and Murakami, A., "Ramjet-Mode Operation in a Scramjet Combustor," ISABE Paper 2003-1150, Sep. 2003.
10) Kouchi, T., Mitani, T., Kodera, M. and Masuya, G., "Numerical Experiments of Scramjet Combustion with Boundary-Layer Bleeding," AIAA Paper 2003-7038, 2003.
11) Mitani, T., Sakuranaka, N., Tomioka, S., Izumikawa, M., "Boundary bleeding Devise for Scramjet engines in M4 and M6 flight Conditions", to be submitted to JPP (2003).
12) Kodera, M., Nakahashi, K., Igarashi, Y., Kanda, T., Hiraiwa, T., and Mitani, T., "Numerical Analysis of Scramjet Internal flow by Hybrid Grid Method," *JSME International Journal*, Series B, Vol. 43, No. 3, 2000.
13) Tomioka, S., Kobayashi, K., Kudo, K., Murakami, A., and Mitani, T., "Effects of Injection Configuration on Performance of a Staged Super-

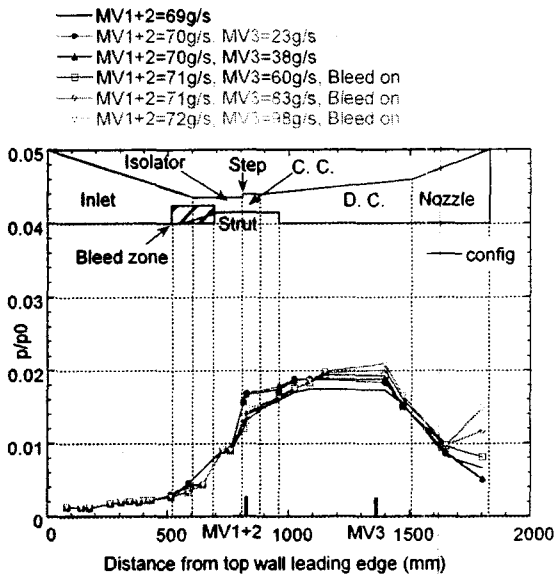

(a) Centerline of top wall

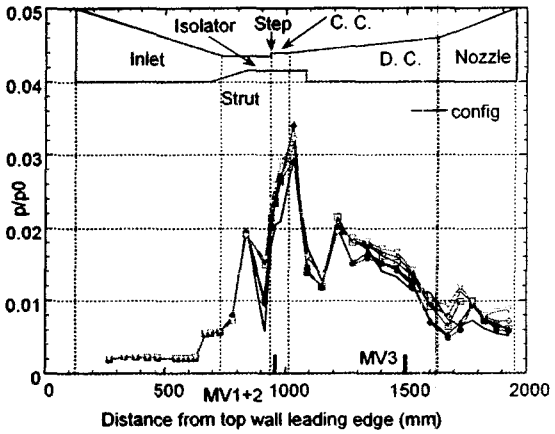

(b) Centerline of side wall

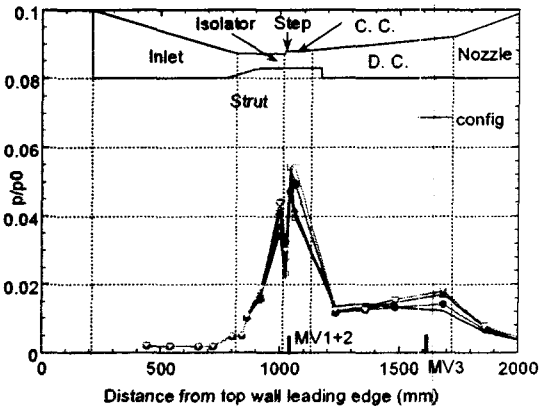

(c) Line close to cowl on side wall

Fig. 8: Wall pressure distributions of two-staged fuel injection at first-stage fuel flow rate of 70 g/s

sonic Combustor," *Journal of Propulsion and Power*, Vol. 19, No. 5, Sep.-Oct. 2003.